Comprehension of Antimicrobial Peptides Modulation of the Type VI Secretion System in *Vibrio cholerae*

Annabelle Mathieu-Denoncourt and Marylise Duperthuy*.

Département de Microbiologie, infectiologie et immunologie, Faculté de médecine, Université de Montréal, Montréal, H3T 1J4, Quebec, Canada.

*Corresponding author: Marylise Duperthuy, Université de Montréal, C.P. 6128, succursale Centre-ville, Montréal, QC, H3C 3J7, tel : 514 343-6111, fax: 514 343-5701, marylise.duperthuy@umontreal.ca

Abstract

The Type VI secretion System (T6SS) is a versatile weapon used by bacteria for virulence, resistance to grazing and competition with other bacteria. We previously demonstrated that the role of the T6SS in interbacterial competition and in resistance to grazing is enhanced in *Vibrio cholerae* in the presence of subinhibitory concentrations of polymyxin B (PmB). In this study, we performed a global quantitative proteomic analysis by liquid chromatography coupled to mass spectrometry and a transcriptomic analysis by quantitative PCR of the T6SS known regulators in *V. cholerae* grown with and without PmB. The proteome of *V. cholerae* is greatly modified in the presence of PmB at subinhibitory concentrations with more than 39 % of the identified cellular proteins displaying a difference in their abundance, including T6SS-related proteins (Hcp, VasC, TsaB and ClpV). We identified a regulator whose abundance and expression are increased in the presence of PmB, *vxrB*, the response regulator of the two-component system VxrAB. In a *vxrAB* deficient mutant, the expression of *hcp* measured by quantitative PCR, although globally reduced, was not modified in the presence of PmB, confirming its role in *hcp* upregulation with PmB. The upregulation of the T6SS in the presence of PmB appears to be, at least in part, due to the two-component system VxrAB.

Keywords

Vibrio cholerae, Type VI Secretion System, Regulation, Polymyxin B, Proteome, antimicrobial peptides, two-component regulatory systems

Importance

The type VI secretion system is important for bacterial competition, virulence and resistance to grazing by predators. In this study, we investigated the regulation leading to the type VI secretion system activation in the presence of polymyxin B (PmB), an antimicrobial used in veterinary and human health to treat infection caused by multi-resistant Gram-negative bacteria, in *V. cholerae*. In addition to making an overall portrait of the modifications to the proteome, we identified the VxrAB two-component system as the main regulator responsible for this activation. Our results provide evidence that subinhibitory concentrations of antimicrobials are responsible for important modifications of the proteome of pathogenic bacteria, inducing the production of proteins involved in virulence, host colonisation, resistance and environmental survival.

Introduction

Vibrio cholerae is a ubiquitous Gram-negative bacterium found in brackish rivers, coastal water and estuaries, or associated with fishes, shellfishes and zooplankton (1). There are more than 200 serotypes of *V. cholerae*, the O1 and O139 causing the cholera disease. The O1 El Tor biotype is responsible for the 7th ongoing pandemic (2). Cholera is acquired by the consumption of contaminated water or food and is characterized by an acute diarrhea, leading to dehydration and eventually to death if not treated (1). *V. cholerae* is endemic in regions where water sanitation facilities are inadequate and access to drinking water is precarious (2, 3). Many virulence and competition effectors allow *V. cholerae* to cause infections, the most important being the cholera toxin and the toxin co-regulated pilus (4, 5).

The type VI secretion system (T6SS), found in more than 25% of Gram-negative bacteria, has been discovered a decade ago in *V. cholerae* (6). The T6SS is a molecular syringe analogous to T4 bacteriophage. It allows the translocation of various toxic effectors into target neighbouring cells. A contraction event of the VipA/B sheath propels a hemolysin-coregulated protein (Hcp) nanotube that punctures the target cell's envelope (7-9). The effectors have many intracellular targets and modes of action in both eukaryotic and prokaryotic cells, such as disruption of the cytoskeleton by actin cross-linking (10, 11), disruption of the cell membrane (12, 13) and peptidoglycan degradation (14, 15). It makes the T6SS an important weapon against competitor bacteria and predators (12, 13, 16, 17). The T6SS genes are divided in multiple gene clusters, *i.e.* a large cluster (VCA0105-VCA0124) that encodes for the major structural proteins, a protease and the internal regulator *vasH* (VCA0117), and at least 2 auxiliary clusters (VCA0017-VCA0022 and VC1415-VC1421), harbouring *hcp*, *vgrG*, adaptor and effector/immunity proteins (6, 12, 18). The expression of

the T6SS genes is complex and involves different regulators (reviewed in (7)), including *vasH*. VasH orchestrates, along with the alternative sigma factor *rpoN*, the expression of the large and auxiliary clusters (7, 19). Most studies on the T6SS in *V. cholerae* were done with non-O1/non-O139 environmental strains that constitutively secrete through their T6SS. However, the regulation appears to vary between strains and seems to differ in clinical isolates as the secretion needs to be triggered. In clinical isolates, high osmolarity and high cell density, involving the regulators *oscR* and *hapR* respectively, are both required for secretion, even though the T6SS is constitutively expressed and produced (20, 21). Globally, the T6SS regulation also depends on other environmental signals, such as bile (22), nucleosides levels (23) and chitin (24-27) through the chitin competence pathway. The global regulators LonA and TsrA also play a role in T6SS regulation. Cold shocks lead to the production of the regulator *cspV*, which modulates the expression of many genes involved in cold shock response, biofilm formation and to the up-regulation of the T6SS (28, 29). The T6SS is also up-regulated by cell wall damages through the two-component system (TCS) VxrAB (30). Bacteria use TCS, a signal transduction device, to regulate the expression of diverse stress or virulence factors in response to variations in their environment and throughout infection (31). TCS are generally composed of a membrane-bound sensor histidine kinase (HK) and a response regulator (RR), which are activated through subsequent phosphorylation. In most TCS, the detection of stimuli by HK leads to the autophosphorylation of its histidine residue, then to the transphosphorylation of the aspartate residue of the RR (32). The RR acts afterwards as a transcriptional regulator. TCS are implicated in various processes such as virulence, stress response, environmental adaptation, and quorum sensing, among others (33). In *V. cholerae, vxrA* and vxr*B* are encoded on the conserved *vxrABCDE* (VCA0565 - VCA0569) (34). VxrC appears to have an inhibitory role in biofilm formation (30). As for VxrDE, their role is still unknown although it has been

98 suggested that VxrDE have a minor role in *vpsL* expression without affecting the biofilm
99 formation (30). While VxrAB are essential for the colonization of infant mouse model, the
100 contribution of VxrCDE is minor (34).
101
102 Antimicrobial peptides (AMPs) are ubiquitous, small, and mostly cationic peptides produced
103 by bacteria and host cells for competition, prevention of infections, or to control the
104 microbiota (35). AMPs are produced in the gut by the microbiota and host cells, and are
105 effective against a broad range of microorganisms such as viruses, fungi and bacteria (36).
106 AMPs have many cellular targets, but the most common mechanism of action is an
107 electrostatic interaction with the negative bacterial membrane that leads to pore formation, the
108 loss of cytoplasmic content and eventually, cell death (37). Polymyxin B (PmB), a cationic
109 AMP produced by *Paenibacillus polymyxa*, binds to the lipid A portion of the LPS at the
110 outer membrane (38). Polymyxins are commonly used in prevention of infections in
111 veterinary medicine and in the treatment of multidrug resistant infections in human health
112 (39). Since the absorption of polymyxins is low, a high percentage is excreted through urine
113 and can accumulate in the environment, including soil and water (40). Polymyxins can thus be
114 found in subinhibitory concentrations in water (41, 42). Subinhibitory concentrations of
115 AMPs are known to have a modulatory effect on virulence, persistence and resistance factors
116 in Gram-negative bacteria (43, 44), including on *V. cholerae* (45-48). El Tor strains are
117 resistant to PmB conversely to the classical strains they replaced (38).
118
119 We previously demonstrated that subinhibitory concentrations of PmB increase the expression
120 of Hcp, the structural component of the T6SS syringe in a pandemic strain of *V. cholerae*
121 (46). PmB alone was not sufficient to induce the secretion through the T6SS in an O1 El Tor
122 strain in low osmolarity conditions, but increased its production and secretion in a dose

dependant manner. Although it did not increase the resistance of *V. cholerae* to antimicrobial peptides or antibiotics, the increased secretion through the T6SS due to the PmB led to a more efficient elimination of the competitor bacteria *E. coli* and an increased cytotoxicity towards amoebas in a T6SS-dependant manner. Furthermore, the increased expression of both *hcp* genes lets us believe that PmB could act as an activating signal for T6SS production and secretion (44, 46). In this study, we aim to identify the regulatory pathways involved in the over expression and over secretion of Hcp in the presence of subinhibitory concentrations of PmB. A proteomic approach of the cell fraction coupled with a transcriptomic approach using quantitative PCR, allowed to determine that the presence of subinhibitory concentrations of PmB has a complex impact on the proteome of *V. cholerae* and greatly modulates the production of proteins implicated in cellular and metabolic processes, regulation and binding and catalytic activities. Among the proteins that were more abundant in the presence of PmB, we identified VxrB, part of the VxrAB TCS and involved in the T6SS regulation. We further constructed a deficient mutant of *vxrAB* and its Hcp production and expression (*hcp*) were assessed by western blot and quantitative PCR. Our results suggest that *vxrAB* is, at least partly, responsible for the increased expression and secretion of Hcp in the presence of PmB in *V. cholerae*.

Material & methods

Strains used in this study

Vibrio cholerae O1 El Tor strain A1552, an Inaba clinical strain isolated in 1992 from a Peruvian tourist, as well as its T6SS defective isogenic mutant A1552Δ*hcp1-2* were used for this study (20, 49). Bacterial strains obtained by mutagenesis by natural competence as previously described (see below) (50) and plasmids used in this study are listed in Table I. *V. cholerae* strains were grown on LB agar plates at 37°C. Isolated colonies were inoculated in 5

mL LB broth and incubated 16 h at 37°C with agitation. To obtain the final cultures, 100 µL of the bacterial suspension were transferred into 5 mL of LB broth with 2% NaCl (LB-2%NaCl), with or without 3 µg/mL of PmB (Sigma-Aldrich) and incubated at 37°C with agitation until they reached an optical density at 600nm (OD_{600nm}) of 2. When needed, L-arabinose (0.05 % w/v) or antibiotics (chloramphenicol (2 µg/mL), carbenicillin (50 µg/mL)) were added to the media.

Proteomic analysis

Proteomic analysis of the bacterial cells grown with or without PmB (3 µg/mL) was performed by liquid chromatography coupled with tandem mass spectrometry, as described before (46). The cellular fraction of *V. cholerae* A1552 cultures at OD_{600nm} of 2 in LB2%NaCl in the presence or in absence of PmB were analyzed. The experiment was conducted in two biological replicates. The proteins were identified using the genome of *V. cholerae* N16961, a strain very closely related to A1552. The data were analyzed using the Scaffold V.5 software (protein threshold: 99%, with at least two peptides identified and a false discovery rate of 1%) and we removed the proteins identified in only one of the replicates. The proteins with differential abundance were then subjected to a Gene Ontology (GO) term enrichment (51).

Mutant construction and complementation

A1552Δ*vxrAB*::CmR and A1552Δ*cspV*::CmR defective mutants were obtained using the optimized natural competence protocol by Marvig & Blokesch (50). All the PCR amplicons were obtained with Thermo Fisher™ oligonucleotide primers listed in Table II, using Taq DNA Polymerase with Standard buffer from New England Biolabs®, according to the manufacturer's instructions. The chloramphenicol resistance cassette (CmR), with its

173 promoter and terminator from pCas9 CR4 (52) (Table I), was amplified by PCR. Up and
174 downstream regions of target genes of about 1000 bp were amplified from A1552 genomic
175 DNA by PCR using primers adding 15 bp homology to CmR 5' and 3' extremities (Table II).
176 The upstream region, the CmR cassette and the downstream region were bound together by
177 overlap PCR and purified using Monarch DNA Gel extraction kit (New England Biolabs®).
178
179 For the natural transformation, briefly, *V. cholerae* wild type strain A1552 was grown over
180 night in LB at 30°C with agitation. The culture was diluted 1:50 in fresh LB and incubated at
181 30°C until it reached an OD_{600nm} of 0.5. Bacteria were washed by centrifugation at 5500 x *g*
182 for 5 min and suspended in M9 minimal media (Sigma) supplemented with 32 mL of $MgSO_4$
183 1 M and 5.1 mL of $CaCl_2$ 1 M per liter (50). The bacteria were diluted 1:2 in fresh M9 media.
184 Chitin powder (Sigma-Aldrich) was added, and the culture was grown overnight at 30°C with
185 agitation. Two hundred ng of purified PCR amplicon were added to the culture, and the
186 bacteria were further incubated 24 h at 30°C. To detach the bacteria from chitin, fresh M9
187 medium was added to the culture and the bacteria were vortexed vigorously for 2 min. The
188 chitin was pelleted by quick centrifugation and the supernatant containing free bacteria was
189 centrifuged at 5000 x *g* for 5 min. The bacteria were suspended in 500 µL of PBS and plated
190 on LB agar supplemented with 2 µg/mL chloramphenicol (Fisher). Plates were incubated at
191 30°C for 3 days. Colonies grown on agar supplemented with chloramphenicol were further
192 isolated on agar plates with chloramphenicol to confirm the phenotype. Deficient mutants
193 were confirmed with PCR using either *cspV* – verif or *vxrAB* – verif primers (Table II) and
194 sequencing of the insertion region.
195
196 For complementation, the complete open reading frame of *cspV* or *vxrAB* was amplified by
197 PCR from purified A1552 genomic DNA using the Thermo Fisher™ oligonucleotide primers

198 adding restriction sites listed in Table II. The amplicons and pBAD24 vector (Table I) were
199 digested using HindIII and EcoRI (*cspV*) or PstI and KpnI (*vxrAB*) from New England
200 Biolabs® according to the manufacturer's instructions. Plasmids and amplicons were purified
201 from agarose gel using Monarch Gel purification kit (New England Biolabs®) and ligated
202 using T4 ligase from New England Biolabs®. The final construction was introduced by heat
203 shock into thermocompetent *E. coli* DH5α at 42°C for 30 s (53). The bacteria were then
204 suspended in fresh LB and incubated 1.5 h at 37°C. Bacteria were selected on LB agar
205 supplemented with carbenicillin (50 µg/mL) (Fisher). Plasmids were extracted from *E. coli*
206 using PureYield™ Plasmid Miniprep System (Promega) and suspended in milliQ water
207 (Thermo Fisher).
208
209 *V. cholerae* was grown in LB for 16 h at 37°C and were made electrocompetent by successive
210 washes in sterile water supplemented with 10% glycerol. The constructions were
211 electroporated in the corresponding strains at 1.275 kV, 25 Ω in 1 mm electroporation
212 cuvettes (Thermo Fisher). The bacteria were incubated 1.5 h at 37°C in LB, then plated on
213 LB agar containing 50 µg/mL carbenicillin. Colonies were screened by PCR using pBAD24 –
214 verif primers (Table II) to verify the construction.
215
216 **Growth curves**
217 *V. cholerae* was grown 16 h at 37 °C with agitation in LB, with carbenicillin when needed. A
218 1:50 dilution in fresh LB was done, and the bacteria were grown at 37°C to an OD_{600nm} of 0.2.
219 Then, 0.05 % L-arabinose was added, and the bacteria were grown until they reached OD_{600nm}
220 = 0.3. They were further diluted 1:50 in LB2%NaCl - 0.05 % L-arabinose, with or without 3
221 µg/mL of PmB, in 50 ml Falcon tubes, or 1:3000 in 96 wells plates. The bacterial growth was

222 followed by reading the OD_{600nm} every 15 min, at 37°C with agitation. Data were obtained
223 from at least three independent experiments, in technical triplicates.
224
225 **RNA extraction, cDNA synthesis and quantitative PCR (RT-qPCR)**
226 *V. cholerae* was grown to an OD_{600nm} of 0.5 at 37°C in 10 mL of LB2%NaCl, with or without
227 3 µg/mL of PmB. The bacteria were suspended in 1 mL TRIzol solution (Invitrogen) and the
228 total RNA was extracted according to the manufacturer's instructions. Five hundred
229 nanograms of RNA were retrotranscribed to cDNA using QuantiNova Reverse Transcription
230 Kit (Qiagen). RNA and cDNA purity and quality were assessed by nanodrop and migration
231 on 2% agarose gel, respectively. Quantitative PCR analysis was done as described before (46)
232 with primers listed in Table II. The relative *hcp* and regulators' expression was calculated in
233 PmB treated bacteria in comparison to non-treated cells using QuantStudio™ Desing and
234 Analysis Software (Thermo Fisher) v1.5.1 and normalized using *recA*. The results were
235 obtained from at least 3 independent experiments, in technical triplicates.
236
237 **Western blot**
238 Bacteria were grown to an OD_{600nm} of 2 in LB2%NaCl, a condition that activates the T6SS
239 secretion in *V. cholerae* A1552, supplemented with – 0.05 % L-arabinose and 3 µg/mL of
240 PmB. Samples were treated and western blot conducted as described before (46). Results are
241 representative of at least three independent experiments.
242
243 **Statistical Analysis**
244 All data are expressed as mean ± SD and were analyzed for significance using the SigmaPlot
245 (version). Student's *t*-tests were used to compare conditions between 2 groups. Single way

ANOVA was used for multiple groups comparison. A result was considered as significant when p value < 0.05 (*).

Results

Proteomic analysis of *V. cholerae*'s cells grown with subinhibitory concentrations of PmB

To identify the cellular proteins whose abundance is modified in the presence of PmB, a quantitative proteomic analysis by liquid chromatography coupled to mass spectrometry was performed on *V. cholerae* A1552 bacterial cells grown in LB2%NaCl with or without 3 µg/ml of PmB, a concentration that does not affect bacterial growth but significantly increases the expression and secretion of Hcp (46). Our proteomic analysis identified a total of 22,819 peptides corresponding to 473 proteins of 7 to 184 kDa. After data curation, 454 proteins were obtained. We calculated the relative abundance of each protein in the presence of PmB in comparison with the control without PmB and determined that 177 proteins (39%) showed a modified abundance in the presence of PmB (Tables IV to VII). Among them, 130 were more abundant in the presence of PmB (Table IV), 17 were less abundant in its presence (Table V), 26 were only found in its presence (Table VI), and 4 were found only in its absence (Table VII). The proteins showing no modulation are presented in Table SI. The correlation of the biological replicates was analyzed using scatter plots and demonstrated a good correlation with R-squared of more than 0.9 (Figure 1AB).

An analysis of the proteins that are modulated by PmB using Go Annotation showed that most modulated proteins have catalytic and/or binding function, with 99 and 75 proteins with these functions, respectively (Figure 1C). Regulatory proteins, transporters, transducers and

sensor proteins were also modulated by PmB. The analysis showed that the proteins that are more abundant in the presence of PmB were mainly implicated in biological (59) and cellular (75) processes (Figure 1C). Regulation, response to stimulus and locomotion were the biological processes that were greatly modified by PmB.

Among the proteins with an increased abundance in the presence of PmB, many have a role in AMPs or PmB resistance (54). For example, VexB, which is part of the efflux system VexAB (55), was 2.7 times more abundant in the presence of PmB, and AlmG and AlmE, which are directly responsible for PmB resistance by LPS modification (56), were 15 and 3.8 times more abundant with PmB, respectively (Table IV). VprB, only present in the presence of PmB (Table VI), is part of the TCS VprAB that activates the expression of AlmGE (57). The protease DegS was also 2.3 times more abundant in the presence of PmB (Table IV). It is responsible for the activation of the alternate sigma factor RpoE, which activates the repair of AMPs induced damages in the bacterial envelope (58). VarF is part of an antibiotic efflux pump (59) and is only found in the presence of PmB (Table VI). OmpR, the RR to the EnvR-OmpR TCS, is a repressor of virulence factors in response to stress envelope, was also more abundant in the presence of PmB (Table IV) (60).

As for the T6SS related proteins, many showed an increased abundance in the presence of PmB, although a lot of the structural components were not identified in our analysis. As expected, the main component of the T6SS syringe, Hcp (VC_1415, VC_A0017), was also more abundant (2.3 times) in the presence of PmB (46). VasC (VC_A0112), a cytoplasmic protein with an FHA domain essential for secretion (61), and ClpV (VC_A0116), the ATPase responsible for recycling of the contractile sheath, presented abundances that were 2.7 and 3.0 times higher in the presence of PmB, respectively. The abundance of VasK (VC_A0120), a

296 part of the inner-membrane complex (62) was increased by 5.5 times by PmB (Table IV).
297 TsaB (VC_1989), the immunity protein to the VgrG-3 that targets the peptidoglycan, had an
298 increased abundance (2.0 times) in the presence of PmB (Table IV). The abundance of VipA
299 (VC_A0107) and VipB (VC_A0108), the small and large subunits of the contractile sheath,
300 was not modified by PmB (Table S1).
301
302 We paid a particular attention to the effect of PmB on the T6SS known regulators. As shown
303 in the table III, our proteomic analysis identified many of them. The abundance of most of
304 these regulators was not significantly affected by the presence of PmB, except for VxrB that
305 was 2.7 times more abundant in the presence of PmB (Table III).
306
307 **Transcriptomic analysis of known T6SS regulators in the presence of PmB**
308 To confirm the results obtained in the proteomic analysis and to include regulators that were
309 not identified in this analysis, we performed a transcriptomic analysis of all the known T6SS
310 regulators of *V. cholerae* A1552 grown in LB2%NaCl supplemented or not with 3 µg/ml of
311 PmB. To do so, a quantitative PCR approach was used and the relative expression of known
312 T6SS regulators was calculated by comparing the number of transcripts from bacterial cells
313 grown with and without PmB and normalized with *recA* (Figure 2A). Although statistically
314 significant, the expression of cyclic AMP receptor protein (CRP) (1.23x), *tfoY* (1.15x), *tsrA*
315 (1.17x) and *osrC* (1.26x) was only slightly higher in the presence of PmB, and was not
316 considered for further analysis. Interestingly, the expression of *vxrB* was 2.1 times higher in
317 the presence of PmB than in its absence, while the expression of *cspV* was decreased by 2.43
318 times in its presence.
319

We also assessed the expression of 2 genes encoding structural proteins of the T6SS, the main component of the contractile sheath, VipB, and ClpV, the ATPase protein responsible for the recycling of the sheath after a contraction event (Figure 2B) (63, 64). Our results showed that the expression of *vipB* is not modified by PmB (Figure 2B). This result is in line with our previous work and the proteomic analysis of this study that showed no difference in protein abundance in the bacterial cell (46). The expression of *clpV* is 1.54 times higher in the presence of PmB (Figure 2B), which is also in line with our proteomic analysis.

Based on the results of both proteomic and transcriptomic analysis showing an increased abundance and expression of VxrB and *vxrB*, respectively, in the presence of PmB, and a decreased expression of *cspV* in the presence of PmB, we constructed defective mutants of the regulators *vxrAB* and *cspV* using natural competence (50) and complemented strains using pBAD24 vector (65). The deletion of *vxrAB* (Figure S1A) or *cspV* (Figure S2A) had no major consequence on bacterial growth. The growth was slightly impaired by complementation and PmB for A1552Δ*vxrAB*::CmR (Figure S1B), but not for A1552Δ*cspV*::CmR (Figure S2B). Like A1552, A1552Δ*cspV*::CmR and A1552Δ*vxrAB*::CmR grew in the presence of PmB at a concentration up to 100 ug/ml, although the growth of A1552Δ*vxrAB*::CmR was impaired in all PmB conditions (result not shown), an observation in line with previous studies (66).

Quantitative PCR analysis of *hcp* shows that *vxrAB,* but not *cspV,* is responsible for its upregulation in the presence of PmB

To determine the effect of the *vxrAB* and *cspV* deletion on the regulation of *hcp* in the presence of PmB, we performed a quantitative PCR analysis. *V. cholerae* A1552, A1552Δ*cspV*::CmR and A1552Δ*vxrAB*::CmR were grown in LB2%NaCl with or without PmB. We quantified the expression of *hcp1* or *hcp2* by quantitative PCR in the presence of

PmB, in comparison to the non-treated cells, and normalized using *recA* (Figure 3 and S3). The expression of *hcp1* and *hcp2* in A1552 treated with PmB was 3.03 and 2.16 times higher, respectively, similarly to what we observed before (46) (Figure 3). For A1552Δ*cspV*::CmR, the expression of *hcp1* and *hcp2* is similar to the wildtype strain, and an upregulation of both *hcp1* and *hcp2* is still observed in the presence of PmB (Figure S3)., indicating that, upon *cspV* mutation, the T6SS is activated by PmB. However, upon *vxrAB* mutation, the expression of *hcp1* and *-2* was significantly reduced, as expected (34), but was not increased in the presence of PmB (Figure 3), indicating that the upregulation due to the PmB is no longer effective.

The secretion of Hcp in A1552 pBAD24, A1552Δ*vxrAB*::CmR pBAD24 and the complemented strain A1552Δ*vxrAB*::CmR pBAD24-*vxrAB* in the presence of PmB was assessed by western blot (Figure 3C). We previously demonstrated that Hcp secretion by *V. cholerae* A1552 is active in the presence of PmB (46). As expected, the secretion of Hcp is greatly reduced upon *vxrAB* mutation (Figure 3C). However, a *vxrAB* complementation completely restored, or even slightly increased, the secretion of Hcp to the level of the WT in the presence of PmB (Figure 3C).

Discussion

In this study, we aim to determine the impact of subinhibitory concentrations of PmB on the proteome of *V. cholerae* and to identify the regulatory pathways involved in the over expression and over secretion of Hcp in the presence of subinhibitory concentrations of PmB. To do so, we performed a proteomic analysis of the cellular fraction of *V. cholerae* O1 El Tor strain A1552 in the presence and in absence of PmB. We identified a total of 22,819 peptides

corresponding to 454 proteins of 7 to 184 kDa, of which 177 had a modified abundance in the presence of PmB.

Several proteins were identified in both our last and current proteomic analysis. It is the case of Hcp that is more abundant in supernatant and bacterial cells in the presence of PmB, and of the proteases VesC and DegP, which was expected since they are secreted components. VesC is secreted through the Type II Secretion System (67), while DegP is secreted by membrane vesicles (68). A putative hydrolase (VC_1485) and an immunogenic protein (VC_0430) were also more abundant in both analysis in the presence of PmB. While the abundance of the lipoprotein Lpp and SucD (α subunit of succinyl-CoA synthetase) was decreased by PmB in the secretome, they were more abundant in the cell fraction. Two proteins were only present in the supernatant in the presence of PmB, and more abundant in the cellular fraction, the amino-acid transporter VC_0010 and the uncharacterized protein VC_0483. One protein, VxrD, was less abundant in both supernatant and bacterial cells in the presence of PmB. Our results show that *V. cholerae* modulates a large proportion of its components in response to PmB, as 39% of the identified proteins had their abundance modified in its presence. Most modulated proteins with increased abundance are implicated in cellular and metabolic processes, with binding, catalytic or transporter activities, that suggests an adaptation to survive the presence of the toxic AMP. This is further supported by the upregulation of efflux systems (VexAB, VprAB, VarF), LPS modifying enzymes (AlmGE), proteases (DegS) and RpoE activating proteins, all known mechanisms of antimicrobials resistance. Numerous proteins displaying a modified abundance in the presence of PmB are yet to be described.

Our previous study has shown that Hcp, the T6SS syringe major component, was more abundant in the secretome of *V. cholerae* under PmB activation (46). The Hcp syringe is

wrapped by the contractile sheath composed of multiple helical polymers of VipAB, assembled in an extended form (69-71). This extended form provides enough energy, upon a contraction signal, for a contraction and rotation of VipAB helical polymers that propel the Hcp syringe, along with the effectors, through the bacterial envelope. Based on the fact that, conversely to the Hcp secreted protein, the abundance of VipB, a structural recycled component of the T6SS, was not modified, we hypothesized that PmB might increase the secretion through the T6SS rather than the number of assembled systems at the bacterial surface. Our current proteomic analysis of bacterial cells confirms that the contractile sheath components VipA and VipB are not more abundant in the presence of PmB. ClpV is a AAA+ (ATPases associated with various cellular activities) that hydrolyzes ATP to reshape, or recycle, various substrates (71). In *V. cholerae*, ClpV recognizes the contracted state of the T6SS sheath and forces its disassembly by unfolding VipB (70). To our knowledge, VipA/B are the only recycled proteins through ClpV activity. The recycling of the contractile sheath is essential and facilitates the effectors' secretion because it makes VipA/B available for further secretion (70, 72). The presence of more ClpV could help the contractile sheath recycling in a cell with a T6SS activated by PmB.

Our proteomic analysis also revealed that the immunity protein TsaB (14, 73), the inner-membrane complex subunit VasK (74), and the FHA protein VasC (TagH), required for secretion (61), are more abundant in the presence of PmB. VasK (TssM) is part of the inner-membrane complex (74) along with VasF (TssL) and VasD (TssJ), a complex randomly distributed in the membrane. Once the inner-membrane complex is formed, it recruits the base plate components, then the Hcp syringe along with the VipA/B sheath (75). It has been suggested that the inner-membrane complexes are pre-assembled in the membrane, more abundant than the syringe portion and that they are reused for further secretion events using new syringe complexes (74). Altogether, our results suggest that more T6SS anchoring

420 complexes might be formed and ready for secretion, while the recycled components
421 abundance remains constant, and the secreted effectors are more produced to increase the
422 number of contraction events and the global T6SS activity in the presence of PmB.
423
424 Our proteomic analysis identified many known regulators of the T6SS in *V. cholerae*, *i.e.*
425 CytR, CRP, TfoY, RpoN, TsrA, OscR and VxrB, but only VxrB had a modified abundance in
426 the presence of PmB. The expression of *crp*, *tfoY*, *tsrA* and *oscR*, although significantly
427 higher, was only slightly modified by PmB, while the expression of *cytR* and *rpoN* was
428 similar to the control. OscR is a transcriptional regulator that represses T6SS genes expression
429 at low osmolarity (21). CytR is activated upon nucleosides starvation, that further activates
430 the expression of T6SS (23). RpoN, along with the internal regulator VasH, coordinates the
431 expression of the different T6SS genes clusters (6). TsrA is a global regulator (76), while
432 TfoY and CRP are produced in response to c-di-GMP and cyclic-AMP, respectively. While
433 CspV was not identified in our proteomic analysis, our transcriptomic results showed that
434 PmB decreases the expression of *cspV*. However, since its expression is reduced in the
435 presence of PmB and known to be produced upon cold shock (29), it is not surprising that it
436 was not identified in the proteomic analysis. We constructed a mutant in which *cspV* is
437 deleted and compared the expression of *hcp1* and *hcp2* in absence and in the presence of PmB
438 for the wild-type strain and the *cspV* mutant. The expression pattern of both *hcp* genes was
439 similar for the two strains, thus suggesting that *cspV* is not responsible for the increased *hcp*
440 expression in the presence of PmB.
441
442 Our proteomic and transcriptomic analysis showed that the presence of PmB increased the
443 production and expression of VxrB, the response regulator of the two-component system
444 VxrAB (34). VxrB is a known regulator of *V. cholerae* T6SS, as its deletion decreases the

445 expression of many T6SS related genes, including Hcp (34). In this study, we constructed a
446 A1552Δ*vxrAB*::CmR mutant, the only essential components of the *vxrABCDE* locus, and a
447 complemented strain. As previously reported, the deletion of *vxrAB* strongly diminished *hcp*
448 expression (34). The complementation of *vxrAB* using pBAD24 restored the secretion of Hcp
449 in the presence of PmB. Conversely to the wild type strain, the presence of PmB did not
450 increase *hcp* expression in A1552Δ*vxrAB*::CmR, demonstrating that it is implicated in the
451 upregulation of *hcp* in the presence of PmB. VxrAB (also known as WigKR) was first
452 identified for its implication in colonization in the infant mouse model and T6SS regulation
453 (34). VxrAB has already been described to regulate other systems implicated in antimicrobial
454 resistance, such as biofilm formation, motility and cell shape maintenance and homeostasis in
455 the presence of cell wall targeting antimicrobials (30, 66, 77). In the later, they demonstrated
456 that the expression of *vxrAB* is increased by antibiotic-induced cell wall damage, and that
457 VxrAB regulates the entire cell wall synthesis pathway, leading to *V. cholerae*'s tolerance to
458 antibiotics (66). Even though we detected no major damages in the cell wall of *V. cholerae*
459 A1552 at a concentration of PmB as high as 25 µg/mL (47), we observed, in this study, a
460 significant upregulation of *vxrB* in the presence of 3 µg/mL of PmB. Taken together, our
461 results suggest that in *V. cholerae* O1 El Tor the T6SS is up regulated by PmB, and that the
462 upregulation involves the TCS VxrAB. The over production of ClpV and VasK also suggests
463 that the T6SS are more efficiently recycled to facilitate the secretion of effectors.
464
465 **Acknowledgment**
466
467 The authors would like to thank Dre Wai from Laboratory for Molecular Infection Medicine
468 Sweden (MIMS) at Umeå University for bacterial strains and the RAQ (Ressources
469 Aquatiques Québec), an inter-institutional group supported financially by the Fonds de

470 recherche du Québec – Nature et technologies (FRQNT) for their support. The proteomic
471 analysis was performed by the Center for Advanced Proteomics Analyses, a Node of the
472 Canadian Genomic Innovation Network supported by the Canadian Government through
473 Genome Canada. This work was supported by the Natural Sciences and Engineering Research
474 Council of Canada (NSERC; http://www.nserc-crsng.gc.ca/index_eng.asp) Discovery grant
475 number RGPIN-2017-05322. AM-D received financial support from the NSERC scholarship
476 program (BESC D3 – 558624 – 2021).
477

Bibliography

1. Harris JB, LaRocque RC, Qadri F, Ryan ET, Calderwood SB. Cholera. Lancet. 2012;379(9835):2466-76.
2. Deen J, Mengel MA, Clemens JD. Epidemiology of cholera. Vaccine. 2020;38 Suppl 1:A31-A40.
3. Jutla A, Whitcombe E, Hasan N, Haley B, Akanda A, Huq A, et al. Environmental factors influencing epidemic cholera. Am J Trop Med Hyg. 2013;89(3):597-607.
4. Vanden Broeck D, Horvath C, De Wolf MJ. Vibrio cholerae: cholera toxin. Int J Biochem Cell Biol. 2007;39(10):1771-5.
5. Mathieu-Denoncourt A, Giacomucci S, Duperthuy M. The Secretome of Vibrio cholerae. In: Huang L, Li J, editors. Vibrios2021.
6. Pukatzki S, Ma AT, Sturtevant D, Krastins B, Sarracino D, Nelson WC, et al. Identification of a conserved bacterial protein secretion system in Vibrio cholerae using the Dictyostelium host model system. Proc Natl Acad Sci U S A. 2006;103(5):1528-33.
7. Joshi A, Kostiuk B, Rogers A, Teschler J, Pukatzki S, Yildiz FH. Rules of Engagement: The Type VI Secretion System in Vibrio cholerae. Trends Microbiol. 2017;25(4):267-79.
8. Crisan CV, Hammer BK. The Vibrio cholerae type VI secretion system: toxins, regulators and consequences. Environ Microbiol. 2020;22(10):4112-22.
9. Unterweger D, Kostiuk B, Otjengerdes R, Wilton A, Diaz-Satizabal L, Pukatzki S. Chimeric adaptor proteins translocate diverse type VI secretion system effectors in Vibrio cholerae. EMBO J. 2015;34(16):2198-210.
10. Pukatzki S, Ma AT, Revel AT, Sturtevant D, Mekalanos JJ. Type VI secretion system translocates a phage tail spike-like protein into target cells where it cross-links actin. Proc Natl Acad Sci U S A. 2007;104(39):15508-13.
11. Durand E, Derrez E, Audoly G, Spinelli S, Ortiz-Lombardia M, Raoult D, et al. Crystal structure of the VgrG1 actin cross-linking domain of the Vibrio cholerae type VI secretion system. J Biol Chem. 2012;287(45):38190-9.
12. Zheng J, Ho B, Mekalanos JJ. Genetic analysis of anti-amoebae and anti-bacterial activities of the type VI secretion system in Vibrio cholerae. PLoS One. 2011;6(8):e23876.
13. Miyata ST, Kitaoka M, Brooks TM, McAuley SB, Pukatzki S. Vibrio cholerae requires the type VI secretion system virulence factor VasX to kill Dictyostelium discoideum. Infect Immun. 2011;79(7):2941-9.
14. Brooks TM, Unterweger D, Bachmann V, Kostiuk B, Pukatzki S. Lytic activity of the Vibrio cholerae type VI secretion toxin VgrG-3 is inhibited by the antitoxin TsaB. J Biol Chem. 2013;288(11):7618-25.
15. Altindis E, Dong T, Catalano C, Mekalanos J. Secretome analysis of Vibrio cholerae type VI secretion system reveals a new effector-immunity pair. mBio. 2015;6(2):e00075.
16. MacIntyre DL, Miyata ST, Kitaoka M, Pukatzki S. The Vibrio cholerae type VI secretion system displays antimicrobial properties. Proc Natl Acad Sci U S A. 2010;107(45):19520-4.
17. Drebes Dorr NC, Blokesch M. Interbacterial competition and anti-predatory behaviour of environmental Vibrio cholerae strains. Environ Microbiol. 2020;22(10):4485-504.
18. Crisan CV, Chande AT, Williams K, Raghuram V, Rishishwar L, Steinbach G, et al. Analysis of Vibrio cholerae genomes identifies new type VI secretion system gene clusters. Genome Biol. 2019;20(1):163.
19. Kitaoka M, Miyata ST, Brooks TM, Unterweger D, Pukatzki S. VasH is a transcriptional regulator of the type VI secretion system functional in endemic and pandemic Vibrio cholerae. J Bacteriol. 2011;193(23):6471-82.
20. Ishikawa T, Rompikuntal PK, Lindmark B, Milton DL, Wai SN. Quorum sensing regulation of the two hcp alleles in Vibrio cholerae O1 strains. PLoS One. 2009;4(8):e6734.

21. Ishikawa T, Sabharwal D, Bröms J, Milton DL, Sjöstedt A, Uhlin BE, et al. Pathoadaptive conditional regulation of the type VI secretion system in Vibrio cholerae O1 strains. Infect Immun. 2012;80(2):575-84.
22. Bachmann V, Kostiuk B, Unterweger D, Diaz-Satizabal L, Ogg S, Pukatzki S. Bile Salts Modulate the Mucin-Activated Type VI Secretion System of Pandemic Vibrio cholerae. PLoS Negl Trop Dis. 2015;9(8):e0004031.
23. Watve SS, Thomas J, Hammer BK. CytR Is a Global Positive Regulator of Competence, Type VI Secretion, and Chitinases in Vibrio cholerae. PLoS One. 2015;10(9):e0138834.
24. Borgeaud S, Metzger LC, Scrignari T, Blokesch M. The type VI secretion system of Vibrio cholerae fosters horizontal gene transfer. Science. 2015;347(6217):63-7.
25. Lo Scrudato M, Blokesch M. A transcriptional regulator linking quorum sensing and chitin induction to render Vibrio cholerae naturally transformable. Nucleic Acids Res. 2013;41(6):3644-58.
26. Meibom KL, Blokesch M, Dolganov NA, Wu CY, Schoolnik GK. Chitin induces natural competence in Vibrio cholerae. Science. 2005;310(5755):1824-7.
27. Metzger LC, Stutzmann S, Scrignari T, Van der Henst C, Matthey N, Blokesch M. Independent Regulation of Type VI Secretion in Vibrio cholerae by TfoX and TfoY. Cell Rep. 2016;15(5):951-8.
28. Townsley L, Sison Mangus MP, Mehic S, Yildiz FH. Response of Vibrio cholerae to Low-Temperature Shifts: CspV Regulation of Type VI Secretion, Biofilm Formation, and Association with Zooplankton. Appl Environ Microbiol. 2016;82(14):4441-52.
29. Datta PP, Bhadra RK. Cold shock response and major cold shock proteins of Vibrio cholerae. Appl Environ Microbiol. 2003;69(11):6361-9.
30. Teschler JK, Cheng AT, Yildiz FH. The Two-Component Signal Transduction System VxrAB Positively Regulates Vibrio cholerae Biofilm Formation. J Bacteriol. 2017;199(18).
31. . !!! INVALID CITATION !!! (73, 74).
32. Kamal F, Liang X, Manera K, Pei TT, Kim H, Lam LG, et al. Differential Cellular Response to Translocated Toxic Effectors and Physical Penetration by the Type VI Secretion System. Cell Rep. 2020;31(11):107766.
33. Krell T, Lacal J, Busch A, Silva-Jimenez H, Guazzaroni ME, Ramos JL. Bacterial sensor kinases: diversity in the recognition of environmental signals. Annu Rev Microbiol. 2010;64:539-59.
34. Cheng AT, Ottemann KM, Yildiz FH. Vibrio cholerae Response Regulator VxrB Controls Colonization and Regulates the Type VI Secretion System. PLoS Pathog. 2015;11(5):e1004933.
35. Boparai JK, Sharma PK. Mini Review on Antimicrobial Peptides, Sources, Mechanism and Recent Applications. Protein Pept Lett. 2020;27(1):4-16.
36. Bevins CL, Salzman NH. Paneth cells, antimicrobial peptides and maintenance of intestinal homeostasis. Nat Rev Microbiol. 2011;9(5):356-68.
37. Le CF, Fang CM, Sekaran SD. Intracellular Targeting Mechanisms by Antimicrobial Peptides. Antimicrob Agents Chemother. 2017;61(4).
38. Matson JS, Yoo HJ, Hakansson K, Dirita VJ. Polymyxin B resistance in El Tor Vibrio cholerae requires lipid acylation catalyzed by MsbB. J Bacteriol. 2010;192(8):2044-52.
39. Trimble MJ, Mlynarcik P, Kolar M, Hancock RE. Polymyxin: Alternative Mechanisms of Action and Resistance. Cold Spring Harb Perspect Med. 2016;6(10).
40. Couet W, Gregoire N, Gobin P, Saulnier PJ, Frasca D, Marchand S, et al. Pharmacokinetics of colistin and colistimethate sodium after a single 80-mg intravenous dose of CMS in young healthy volunteers. Clin Pharmacol Ther. 2011;89(6):875-9.
41. Serwecinska L. Antimicrobials and Antibiotic-Resistant Bacteria: A Risk to the Environment and to Public Health. Water. 2020;12(12):3313.
42. Davis CA, Janssen EM. Environmental fate processes of antimicrobial peptides daptomycin, bacitracins, and polymyxins. Environ Int. 2020;134:105271.
43. Duperthuy M. Antimicrobial Peptides: Virulence and Resistance Modulation in Gram-Negative Bacteria. Microorganisms. 2020;8(2).
44. Linares JF, Gustafsson I, Baquero F, Martinez JL. Antibiotics as intermicrobial signaling agents instead of weapons. Proc Natl Acad Sci U S A. 2006;103(51):19484-9.

579 45. Duperthuy M, Sjöström AE, Sabharwal D, Damghani F, Uhlin BE, Wai SN. Role of the Vibrio
580 cholerae matrix protein Bap1 in cross-resistance to antimicrobial peptides. PLoS Pathog.
581 2013;9(10):e1003620.
582 46. Mathieu-Denoncourt A, Duperthuy M. Secretome analysis reveals a role of subinhibitory
583 concentrations of polymyxin B in the survival of Vibrio cholerae mediated by the type VI secretion
584 system. Environ Microbiol. 2022;24(3):1133-49.
585 47. Giacomucci S, Cros CD, Perron X, Mathieu-Denoncourt A, Duperthuy M. Flagella-dependent
586 inhibition of biofilm formation by sub-inhibitory concentration of polymyxin B in Vibrio cholerae.
587 PLoS One. 2019;14(8):e0221431.
588 48. Giacomucci S, Mathieu-Denoncourt A, Vincent AT, Jannadi H, Duperthuy M. Experimental
589 evolution of Vibrio cholerae identifies hypervesiculation as a way to increase motility in the presence
590 of polymyxin B. Front Microbiol. 2022.
591 49. Allue-Guardia A, Echazarreta M, Koenig SSK, Klose KE, Eppinger M. Closed Genome Sequence
592 of Vibrio cholerae O1 El Tor Inaba Strain A1552. Genome Announc. 2018;6(9).
593 50. Marvig RL, Blokesch M. Natural transformation of Vibrio cholerae as a tool--optimizing the
594 procedure. BMC Microbiol. 2010;10:155.
595 51. Thomas PD, Campbell MJ, Kejariwal A, Mi H, Karlak B, Daverman R, et al. PANTHER: a library
596 of protein families and subfamilies indexed by function. Genome Res. 2003;13(9):2129-41.
597 52. Reisch CR, Prather KL. The no-SCAR (Scarless Cas9 Assisted Recombineering) system for
598 genome editing in Escherichia coli. Sci Rep. 2015;5:15096.
599 53. Chang AY, Chau VW, Landas JA, Pang Y. Preparation of calcium competent Escherichia coli
600 and

601 heat-shock transformation UJEMI. 2017;1:22-5.
602 54. Conner JG, Teschler JK, Jones CJ, Yildiz FH. Staying Alive: Vibrio cholerae's Cycle of
603 Environmental Survival, Transmission, and Dissemination. Microbiol Spectr. 2016;4(2).
604 55. Bina JE, Provenzano D, Wang C, Bina XR, Mekalanos JJ. Characterization of the Vibrio
605 cholerae vexAB and vexCD efflux systems. Arch Microbiol. 2006;186(3):171-81.
606 56. Henderson JC, Herrera CM, Trent MS. AlmG, responsible for polymyxin resistance in
607 pandemic Vibrio cholerae, is a glycyltransferase distantly related to lipid A late acyltransferases. J Biol
608 Chem. 2017;292(51):21205-15.
609 57. Herrera CM, Crofts AA, Henderson JC, Pingali SC, Davies BW, Trent MS. The Vibrio cholerae
610 VprA-VprB two-component system controls virulence through endotoxin modification. mBio.
611 2014;5(6).
612 58. Mathur J, Waldor MK. The Vibrio cholerae ToxR-regulated porin OmpU confers resistance to
613 antimicrobial peptides. Infect Immun. 2004;72(6):3577-83.
614 59. Lin HV, Massam-Wu T, Lin CP, Wang YA, Shen YC, Lu WJ, et al. The Vibrio cholerae var
615 regulon encodes a metallo-beta-lactamase and an antibiotic efflux pump, which are regulated by
616 VarR, a LysR-type transcription factor. PLoS One. 2017;12(9):e0184255.
617 60. Kunkle DE, Bina TF, Bina XR, Bina JE. Vibrio cholerae OmpR Represses the ToxR Regulon in
618 Response to Membrane Intercalating Agents That Are Prevalent in the Human Gastrointestinal Tract.
619 Infect Immun. 2020;88(3).
620 61. Wang G, Fan C, Wang H, Jia C, Li X, Yang J, et al. Type VI secretion system-associated FHA
621 domain protein TagH regulates the hemolytic activity and virulence of Vibrio cholerae. Gut Microbes.
622 2022;14(1):2055440.
623 62. Nazarov S, Schneider JP, Brackmann M, Goldie KN, Stahlberg H, Basler M. Cryo-EM
624 reconstruction of Type VI secretion system baseplate and sheath distal end. EMBO J. 2018;37(4).
625 63. Kapitein N, Bonemann G, Pietrosiuk A, Seyffer F, Hausser I, Locker JK, et al. ClpV recycles
626 VipA/VipB tubules and prevents non-productive tubule formation to ensure efficient type VI protein
627 secretion. Mol Microbiol. 2013;87(5):1013-28.

64. Kube S, Kapitein N, Zimniak T, Herzog F, Mogk A, Wendler P. Structure of the VipA/B type VI secretion complex suggests a contraction-state-specific recycling mechanism. Cell Rep. 2014;8(1):20-30.
65. Guzman LM, Belin D, Carson MJ, Beckwith J. Tight regulation, modulation, and high-level expression by vectors containing the arabinose PBAD promoter. J Bacteriol. 1995;177(14):4121-30.
66. Dorr T, Alvarez L, Delgado F, Davis BM, Cava F, Waldor MK. A cell wall damage response mediated by a sensor kinase/response regulator pair enables beta-lactam tolerance. Proc Natl Acad Sci U S A. 2016;113(2):404-9.
67. Sikora AE, Zielke RA, Lawrence DA, Andrews PC, Sandkvist M. Proteomic analysis of the Vibrio cholerae type II secretome reveals new proteins, including three related serine proteases. J Biol Chem. 2011;286(19):16555-66.
68. Altindis E, Fu Y, Mekalanos JJ. Proteomic analysis of Vibrio cholerae outer membrane vesicles. Proc Natl Acad Sci U S A. 2014;111(15):E1548-56.
69. Broms JE, Ishikawa T, Wai SN, Sjostedt A. A functional VipA-VipB interaction is required for the type VI secretion system activity of Vibrio cholerae O1 strain A1552. BMC Microbiol. 2013;13:96.
70. Kudryashev M, Wang RY, Brackmann M, Scherer S, Maier T, Baker D, et al. Structure of the type VI secretion system contractile sheath. Cell. 2015;160(5):952-62.
71. Bonemann G, Pietrosiuk A, Diemand A, Zentgraf H, Mogk A. Remodelling of VipA/VipB tubules by ClpV-mediated threading is crucial for type VI protein secretion. EMBO J. 2009;28(4):315-25.
72. Pietrosiuk A, Lenherr ED, Falk S, Bonemann G, Kopp J, Zentgraf H, et al. Molecular basis for the unique role of the AAA+ chaperone ClpV in type VI protein secretion. J Biol Chem. 2011;286(34):30010-21.
73. Miyata ST, Unterweger D, Rudko SP, Pukatzki S. Dual expression profile of type VI secretion system immunity genes protects pandemic Vibrio cholerae. PLoS Pathog. 2013;9(12):e1003752.
74. Durand E, Nguyen VS, Zoued A, Logger L, Pehau-Arnaudet G, Aschtgen MS, et al. Biogenesis and structure of a type VI secretion membrane core complex. Nature. 2015;523(7562):555-60.
75. Stietz MS, Liang X, Li H, Zhang X, Dong TG. TssA-TssM-TagA interaction modulates type VI secretion system sheath-tube assembly in Vibrio cholerae. Nat Commun. 2020;11(1):5065.
76. Zheng J, Shin OS, Cameron DE, Mekalanos JJ. Quorum sensing and a global regulator TsrA control expression of type VI secretion and virulence in Vibrio cholerae. Proc Natl Acad Sci U S A. 2010;107(49):21128-33.
77. Peschek N, Herzog R, Singh PK, Sprenger M, Meyer F, Frohlich KS, et al. RNA-mediated control of cell shape modulates antibiotic resistance in Vibrio cholerae. Nat Commun. 2020;11(1):6067.
78. Liu J, Chang W, Pan L, Liu X, Su L, Zhang W, et al. An Improved Method of Preparing High Efficiency Transformation Escherichia coli with Both Plasmids and Larger DNA Fragments. Indian J Microbiol. 2018;58(4):448-56.
79. Rogers A, Townsley L, Gallego-Hernandez AL, Beyhan S, Kwuan L, Yildiz FH. The LonA Protease Regulates Biofilm Formation, Motility, Virulence, and the Type VI Secretion System in Vibrio cholerae. J Bacteriol. 2016;198(6):973-85.
80. Joshi A, Mahmoud SA, Kim SK, Ogdahl JL, Lee VT, Chien P, et al. c-di-GMP inhibits LonA-dependent proteolysis of TfoY in Vibrio cholerae. PLoS Genet. 2020;16(6):e1008897.

Tables

Table I Bacterial strains and plasmids used in this study

Strain/plasmid	General characteristics	Reference
V. cholerae		
A1552	Wild type strain, O1 El Tor, pathogenic strain isolated from human cholera infection	(49)
A1552Δ*hcp1-2*	Hemolysin coregulated protein (Hcp) expression-deficient strain derived from A1552. Deletion of *hcp* genes from auxiliary clusters 1 and 2. Lacks functional T6SS.	(20)
A1552Δ*vxrAB*::CmR	A1552 derived strain in which *vxrAB* (VCA0565-66) have been replaced by a chloramphenicol resistance cassette, with promoter and terminator, from pCas9 CR4	This study
A1552Δ*cspV*::CmR	A1552 derived strain in which *cspV* (VCA0933) have been replaced by a chloramphenicol resistance cassette, with promoter and terminator, from pCas9 CR4	This study
E. coli		
DH5α	F– φ80*lacZ*ΔM15 Δ(*lacZYA-argF*) U169 *recA*1 *endA*1 *hsdR*17(r_K^-, m_K^+) *phoA supE*44 λ–*thi*-1 *gyrA*96 *relA*1	(78)
Plasmids		
pBAD24	Expression vector. Arabinose inducible promoter, resistance cassette to carbenicillin (https://www.addgene.org/vector-database/1845/)	(65)
pBAD24-*vxrAB*	pBAD24 vector with complete *vxrAB* open reading frame from A1552 under *ara* promotor	This study
pBAD24-*cspV*	pBAD24 vector with complete *cspV* open reading frame from A1552 under *ara* promotor	This study
pCas9 CR4	Cas9 nuclease under control of pTet promoter with *ssrA* tag and constitutive *tetR* (https://www.addgene.org/62655/)	(52)

678 **Table II Primers used in this study**

Mutant construction		
Gene	**Forward**	**Reverse**
CmR	ACGTTGATCGGCACGTAAGAGGTTCCAACTTTCACC	TGGATTCTCACCAATAAAAAACGCCCGGCGGC
vxrAB up	GGCGGCATTAGTCGTTTCTGGCTTATTGCTGAT	CGTGCCGATCAACGTTATCCGGTAAAGAGATATTCGAGTGTTATATTGATGTCAATAATGACA
vxrAB down	GCGTTTTTTATTGGTGAGAATCCAGTGATCATGGTTAAGCCAAATCCTCTTTTATGGTT	GGTTTTGCTAATAACTTGAGATTGTTCAATAGCTAGCGGTCCTTGC
vxrAB - cloning	AGCTGGTACCATGCGTTATAGTTTTTGCATGT	AGCTCTGCAGATCACGCTTTCATTTTGTAACC
vxrAB - verif	TGCAATACTGCACAGCTTTG	GCGTGCTTCAACTGCATAAT
cspV up	CCTTGACCGTTCCAATGCTCATCCAGT	CGTGCCGATCAACGTAGAGACCTCTAGAGATAATTTT
cspV down	ATTGGTGAGAATCCAAGGAATTCATGTCTCGCAGAAC	CATGAAAATGAGTGGACGACAGAAAAC
cspV - cloning	GCCGAGAATTCATGTCTACTAAAATGACTGGTT	AGCTTTCGAATTACAGTGCGACTACGTTAGAC
cspV - verif	TAATCTCTTGCAGGGCTTCT	GGATGAGGCAGACATCATTTCT
pBAD24 - verif	TTGCCGTCACTGCGTCTTT	CCGCTTCTGCGTTCTGATTTA

qPCR		
Gene	**Forward**	**Reverse**
CRP	GTCAAATGGCTCGTCGTCT	GAGTCTGTGCGATACGGC
cspA	CTCAAGACAACGGCGGTC	TTGCCTTGCTCAACGGTG
cspV	ACTCAAGACAACGGTGGCA	GCCTTTCTTACCTTGTTCAACGA
cytR	GCCGAGGTCAGGTTATCAATGT	CAGACGGTATGTTGCTGCTG
hapR	GGAGTAGAAGATGCCGTGGA	CCAACCGAACTAACCAACTGC
lonA	CTTCCGCTTTGACTGGGTTAC	GTGCGACACCTAAAGATGGC
oscR	GCGTATATGGTGCCTGTCG	CGAAGCAGTGGTTGACTTTGAC
rpoN	TCTACGAACCTGAACCGCA	CGCTGTAGACTTCATCCCAAG
tfoX	GAGCAACATCACCCTGAGC	TAGACGACGACTGGCTGCT
tsrA	CGTTCACTGCTTTGATTGCCTA	GCTCGCATTCTGGAACAACT
vxrB	AGATAGTGGGCAAGATGACAG	CGTCGTCGGGAAATGGTTA
vipB	GCGTGAATCGGAAGATGCTCG	CCACAGGTAGTGCTCGTG
clpV	CCTTGTGCCATCAGCGTCA	GCTGCTGCCAACTCTGTGTC
hcp1	CAAACTCAGGGTCTTATCACTGC	GGTCAGTCGGTACAGTCACA
hcp2	ATGTACTGCTGACTCTATCGGC	GTCAGTCGGTACGGTTACG
recA	ATTGAAGGCGAAATGGGCGATAG	TACACATACAGTTGGATTGCTTGAG

679 CmR: chloramphenicol resistance cassette; Up: 1000 bp upstream region; Down: 1000 bp

680 downstream region; CRP, Cyclic AMP receptor protein.

681

682 **Table III Known regulators of the Type VI secretion system of *V. cholerae* identified in**

683 **our proteomic analysis.**

Gene		Found in Analysis	Modified abundance in the presence of PmB	Reference
VC_1021	LuxO	No	NA	(20)
VC_2677	CytR	Yes	No	(23)
VC_1153	TfoX	No	NA	(24, 25, 27)
VC_2614	CRP	Yes	No	(20)
VC_0583	HapR	No	NA	(20, 25)
VC_0396	QstR	No	NA	(24)
VC_1722	TfoY	Yes	No	(27)
VC_0117	VasH	No	NA	(6)
VC_2529	RpoN	Yes	No	(6)
VC_0070	TsrA	Yes	No	(76)
VC_A0566	VxrB	Yes	Increased	(34)
VC_A0933	CspV	No	NA	(28)
VC_A0029	OscR	Yes	No	(21)
VC_1920	LonA	No	NA	(79, 80)

684

685

686 **Table IV. Cellular proteins that are more abundant in the presence of polymyxin B in *V.***
687 ***cholerae* A1552.**

Accession number	Alternate ID		Molecular weight	PmB 3ug/ml #1	PmB 3ug/ml #2	no PmB #1	No PmB #2	Mean 3µg/ml	Mean No PmB	Ratio 3:0
Q9KQG5_VIBCH	VC_2033	AdhE	96 kDa	79	187	62	72	133.0	67.0	2.0
Q9KTZ9_VIBCH	VC_0731	Prdx	23 kDa	39	130	37	38	84.5	37.5	2.3
Q9KUF5_VIBCH	VC_0566	DegP	48 kDa	50	92	27	21	71.0	24.0	3.0
Q9KUT5_VIBCH	VC_0430	Immunogenic protein	35 kDa	48	78	37	25	63.0	31.0	2.0
Q9KNS5_VIBCH	VC_2656	FrdA	66 kDa	54	83	26	40	68.5	33.0	2.1
Q9KUG7_VIBCH	VC_0554	Putative peptidase	106 kDa	50	79	18	12	64.5	15.0	4.3
Q9KV04_VIBCH	VC_0354	FkpA	28 kDa	35	69	25	24	52.0	24.5	2.1
Q9KTF5_VIBCH	VC_0947	DacA	43 kDa	36	56	24	23	46.0	23.5	2.0
Q9KQB6_VIBCH	VC_2084	*sucD*	30 kDa	30	61	25	21	45.5	23.0	2.0
Q9KSG3_VIBCH	VC_1293	AspC	45 kDa	30	61	22	23	45.5	22.5	2.0
Q9KRZ8_VIBCH	VC_1485	Putative hydrolase	61 kDa	34	39	19	18	36.5	18.5	2.0
Q9KNA6_VIBCH	VCA_0059	Lpp	13 kDa	30	48	17	17	39.0	17.0	2.3
Q9KPK3_VIBCH	VC_2364	ThrA	89 kDa	20	32	13	13	26.0	13.0	2.0
Q9KQI5_VIBCH	VC_2013	PtsG	52 kDa	13	34	10	11	23.5	10.5	2.2
Q9KV51_VIBCH	VC_0306	TrxA	12 kDa	11	35	12	7	23.0	9.5	2.4
Q9KRJ1_VIBCH	VC_1649	VesC	60 kDa	11	39	9	11	25.0	10.0	2.5
Q9KVM9_VIBCH	VC_0112	Cytochrome C4	24 kDa	12	33	9	8	22.5	8.5	2.6
Q9KR86_VIBCH	VC_1756	VexC	40 kDa	11	21	7	9	16.0	8.0	2.0
Q9KQ20_VIBCH	VC_2185	*ychF*	42 kDa	11	18	7	7	14.5	7.0	2.1
Q9KQL3_VIBCH	VC_1985	FadD	63 kDa	13	19	7	6	16.0	6.5	2.5
Q9KUV9_VIBCH	VC_0402	MshL	60 kDa	12	16	7	7	14.0	7.0	2.0
Q9KTY7_VIBCH	VC_0743	*secD*	67 kDa	10	22	6	7	16.0	6.5	2.5
Q9KPC9_VIBCH	VC_2443	Hypothetical protein	23 kDa	10	14	5	7	12.0	6.0	2.0
Q9KUE5_VIBCH	VC_0576	SspA	24 kDa	12	14	6	7	13.0	6.5	2.0
Q9KVI2_VIBCH	VC_0164	VexB	112 kDa	10	20	6	5	15.0	5.5	2.7
Q9KMZ1_VIBCH	VC_A0175	MoxR-related protein	35 kDa	11	17	4	2	14.0	3.0	4.7
Q9KU59_VIBCH	VC_0665	VpsR	50 kDa	10	12	7	3	11.0	5.0	2.2
Q9KP11_VIBCH	VC_2568	FklB	22 kDa	8	15	6	4	11.5	5.0	2.3
Q9KQP8_VIBCH	VC_1950	TorZ	89 kDa	11	12	6	4	11.5	5.0	2.3
H9L4Q3_VIBCH	VC_1415	Hcp	19 kDa	10	17	4	8	13.5	6.0	2.3
Q9KUN2_VIBCH	VC_0483	Uncharacterized protein	27 kDa	9	11	4	5	10.0	4.5	2.2
Q9KVW1_VIBCH	VC_0027	*ilvA*	56 kDa	13	13	2	6	13.0	4.0	3.3
Q9KKS3_VIBCH	VC_A1027	*malM*, putative	31 kDa	6	15	3	4	10.5	3.5	3.0
Q9KQY8_VIBCH	VC_1859	Methyl-accepting chemotaxis protein	77 kDa	6	15	5	4	10.5	4.5	2.3
Q9KU34_VIBCH	VC_0695	phospho-2-dehydro-3-deoxyheptonate-aldolase	40 kDa	8	11	3	5	9.5	4.0	2.4
Q9KKJ3_VIBCH	VC_A1114	*parA2*	36 kDa	7	13	1	6	10.0	3.5	2.9
Q9KRS3_VIBCH	VC_1563	VarA	37 kDa	9	9	3	0	9.0	1.5	6.0
Q9KNL8_VIBCH	VC_2714	OmpR	27 kDa	7	13	4	3	10.0	3.5	2.9
Q9KRQ7_VIBCH	VC_1579	AlmE	63 kDa	7	12	1	4	9.5	2.5	3.8

Q9KPD2_VIBCH	VC_2440	Uncharacterized protein	59 kDa	10	10	5	5	10.0	5.0	2.0
Q9KPJ1_VIBCH	VC_2376	GltB	164 kDa	9	13	8	2	11.0	5.0	2.2
Q9KUE3_VIBCH	VC_0578	Putative hemolysin	21 kDa	7	13	1	1	10.0	1.0	10.0
Q9KNB8_VIBCH	VC_A0047	Putative multidrug resistance efflux pump (EmrA)	42 kDa	6	12	2	0	9.0	1.0	9.0
Q9KNP3_VIBCH	VC_2688	GlpX	36 kDa	6	11	4	3	8.5	3.5	2.4
Q9KPM4_VIBCH	VC_2343	*radA*	49 kDa	7	10	5	3	8.5	4.0	2.1
Q9KQK4_VIBCH	VC_1994	*sspA*. Protease IV	67 kDa	4	13	2	4	8.5	3.0	2.8
Q9KS77_VIBCH	VC_1382	HrpA	150 kDa	5	9	5	2	7.0	3.5	2.0
Q9KTT2_VIBCH	VC_0806	Uncharacterized protein	59 kDa	7	9	3	1	8.0	2.0	4.0
Q9KU23_VIBCH	VC_0706	Vrp	12 kDa	3	11	3	3	7.0	3.0	2.3
Q9KTY8_VIBCH	VC_0742	yajC	12 kDa	3	13	5	3	8.0	4.0	2.0
Q9KKJ2_VIBCH	VC_A1115	parB2	46 kDa	5	7	2	1	6.0	1.5	4.0
Q9KVN3_VIBCH	VC_0108	polA	104 kDa	6	7	4	2	6.5	3.0	2.2
Q9KRQ9_VIBCH	VC_1577	AlmG	31 kDa	6	9	1	0	7.5	0.5	15.0
Q9KVS7_VIBCH	VC_0062	*thiE*	49 kDa	4	7	3	2	5.5	2.5	2.2
Q9KSD7_VIBCH	VC_1321	Hypothetical protein	116 kDa	5	9	3	1	7.0	2.0	3.5
Q9KPX3_VIBCH	VC_2239	NprII	13 kDa	3	9	2	4	6.0	3.0	2.0
Q9KTI9_VIBCH	VC_0913	VexG	39 kDa	5	5	3	2	5.0	2.5	2.0
Q9KQD2_VIBCH	VC_2068	FlhF	55 kDa	6	6	2	1	6.0	1.5	4.0
Q9KVX8_VIBCH	VC_0010	Amino acid ABC transporter	27 kDa	3	7	4	1	5.0	2.5	2.0
Q9KM23_VIBCH	VC_A0566	VxrB	28 kDa	4	4	1	2	4.0	1.5	2.7
Q9KUE7_VIBCH	VC_0574	Cytochrome b	48 kDa	6	8	3	4	7.0	3.5	2.0
Q9KS28_VIBCH	VC_1433	Hypothetical protein	35 kDa	5	7	2	3	6.0	2.5	2.4
H9L4Q9_VIBCH	VC_2451	RelA	84 kDa	6	5	1	2	5.5	1.5	3.7
Q9KQ39_VIBCH	VC_2165	ArsC	13 kDa	2	7	1	1	4.5	1.0	4.5
Q9KVF2_VIBCH	VC_0194	gamma-glutamyl transpeptidase	63 kDa	5	6	2	0	5.5	1.0	5.5
Q9KR87_VIBCH	VC_1755	Hypothetical protein	22 kDa	4	4	1	3	4.0	2.0	2.0
Q9KN45_VIBCH	VC_A0120	VasK	135 kDa	5	6	1	1	5.5	1.0	5.5
Q9KNS4_VIBCH	VC_2657	Fumarate reductase	28 kDa	2	6	0	3	4.0	1.5	2.7
Q9KN53_VIBCH	VC_A0112	VasC/Fha	55 kDa	4	4	2	1	4.0	1.5	2.7
Q9KVK8_VIBCH	VC_0134	Hypothetical protein	31 kDa	6	4	2	2	5.0	2.0	2.5
Q9KUU1_VIBCH	VC_0424	rraB	16 kDa	2	5	1	2	3.5	1.5	2.3
Q9KVM5_VIBCH	VC_0116	ClpV	56 kDa	1	8	1	2	4.5	1.5	3.0
Q9KSA9_VIBCH	VC_1350	Peroxiredoxin-2D	17 kDa	2	6	2	2	4.0	2.0	2.0
Q9KT26_VIBCH	VC_1079	Hypothetical protein	36 kDa	4	4	2	2	4.0	2.0	2.0
Q9KKM1_VIBCH	VC_A1082	LapD subunit	43 kDa	4	3	3	0	3.5	1.5	2.3
Q9KP64_VIBCH	VC_2512	Hypothetical protein	14 kDa	4	5	1	2	4.5	1.5	3.0
H9L4Q7_VIBCH	VC_2528	LptB	27 kDa	4	5	1	2	4.5	1.5	3.0
Q9KT57_VIBCH	VC_1048	Hypothetical protein	20 kDa	2	6	2	2	4.0	2.0	2.0
Q9KSQ8_VIBCH	VC_1198	Hypothetical protein	114 kDa	3	5	0	2	4.0	1.0	4.0

Q9KQK9_VIBCH	VC_1989	TsaB	26 kDa	3	5	3	1	4.0	2.0	2.0
Q9KUP6_VIBCH	VC_0469	Ribosomal RNA small subunit methyltransferase E	27 kDa	2	6	1	2	4.0	1.5	2.7
Q9KUD3_VIBCH	VC_0589	Putative ATPAse-ABC transporter	34 kDa	4	3	2	1	3.5	1.5	2.3
Q9KUW7_VIBCH	VC_0392	Aminotransferase. class V	41 kDa	3	3	1	2	3.0	1.5	2.0
Q9KUU3_VIBCH	VC_0422	TldD	51 kDa	3	5	0	4	4.0	2.0	2.0
Q9KM14_VIBCH	VC_A0575	LysR	33 kDa	3	4	0	2	3.5	1.0	3.5
Q9KR78_VIBCH	VC_1765	HsdR putative	117 kDa	3	3	2	0	3.0	1.0	3.0
H9L4P8_VIBCH	VC_A0446	Haemagglutinin	7 kDa	3	5	2	2	4.0	2.0	2.0
Q9KRY0_VIBCH	VC_1503	Hypothetical protein	33 kDa	2	4	1	2	3.0	1.5	2.0
Q9KRZ7_VIBCH	VC_1486	*uup*	72 kDa	3	4	3	0	3.5	1.5	2.3
Q9KU33_VIBCH	VC_0696	*tyrA*	42 kDa	4	4	1	1	4.0	1.0	4.0
Q9KPA8_VIBCH	VC_2465	RseB	36 kDa	3	4	0	1	3.5	0.5	7.0
Q9KSF6_VIBCH	VC_1300	*sdaA-1*	49 kDa	4	3	1	2	3.5	1.5	2.3
Q9KMW7_VIBCH	VC_A0199	DUF262 domain-containing protein	74 kDa	1	4	1	1	2.5	1.0	2.5
Q9KQN4_VIBCH	VC_1964	Hypothetical protein	32 kDa	3	6	0	2	4.5	1.0	4.5
Q9KPY9_VIBCH	VC_2223	Pseudo uridine synthase family 1 protein	38 kDa	2	5	2	0	3.5	1.0	3.5
Q9KNW7_VIBCH	VC_2613	*prkB*	33 kDa	3	2	1	1	2.5	1.0	2.5
Q9KQF4_VIBCH	VC_2044	*ydhD*	12 kDa	3	4	1	2	3.5	1.5	2.3
Q9KUF6_VIBCH	VC_0565	DegS	38 kDa	2	5	0	3	3.5	1.5	2.3
Q9KPR7_VIBCH	VC_2299	*ppiA*	21 kDa	2	3	0	2	2.5	1.0	2.5
Q9KQL1_VIBCH	VC_1987	Slp	23 kDa	2	2	1	1	2.0	1.0	2.0
Q9KP37_VIBCH	VC_2542	*mpl*	49 kDa	2	4	1	1	3.0	1.0	3.0
Q9KQU1_VIBCH	VC_1907	*cysB*	36 kDa	2	3	0	2	2.5	1.0	2.5
Q9KV68_VIBCH	VC_0289	gnt-I transcriptional repressor	36 kDa	2	4	0	1	3.0	0.5	6.0
Q9KUK0_VIBCH	VC_0519	Hypothetical protein	16 kDa	4	3	1	1	3.5	1.0	3.5
Q9KQT9_VIBCH	VC_1909	Hypothetical protein	30 kDa	3	5	0	2	4.0	1.0	4.0
Q9KNG6_VIBCH	VC_2773	*parA* homologue	28 kDa	3	3	1	1	3.0	1.0	3.0
Q9KLA6_VIBCH	VC_A0840	Putative deoxycytidylate deaminase	18 kDa	3	2	0	2	2.5	1.0	2.5
Q9KL30_VIBCH	VC_A0919	Hypothetical protein	11 kDa	3	2	0	1	2.5	0.5	5.0
Q9KM74_VIBCH	VC_A0514	Putative Zn-protease	25 kDa	2	2	1	1	2.0	1.0	2.0
Q9KQP7_VIBCH	VC_1951	*torY*	41 kDa	2	2	1	1	2.0	1.0	2.0
Q9KP72_VIBCH	VC_2504	*hprA*	35 kDa	1	3	1	1	2.0	1.0	2.0
Q9KT28_VIBCH	VC_1077	Hypothetical protein	18 kDa	2	3	0	1	2.5	0.5	5.0
Q9KVB1_VIBCH	VC_0235	*wavJ*	39 kDa	2	3	2	0	2.5	1.0	2.5
H9L4R0_VIBCH	VC_0260	*wbeU*	69 kDa	0	4	1	1	2.0	1.0	2.0
Q9KRI6_VIBCH	VC_1655	*mgtE*	50 kDa	2	4	1	0	3.0	0.5	6.0
Q9KL70_VIBCH	VC_A0877	Putative hydrolase	39 kDa	2	2	0	2	2.0	1.0	2.0
Q9KM44_VIBCH	VC_A0545	5`-nucleotidase.	64 kDa	2	2	1	0	2.0	0.5	4.0

		putative								
Q9KPU2_VIBCH	VC_2270	*ribE*	24 kDa	2	2	1	1	2.0	1.0	2.0
Q9KQ75_VIBCH	VC_2126	FliM	40 kDa	0	2	0	1	1.0	0.5	2.0
Q9KRN0_VIBCH	VC_1606	Hypothetical protein	52 kDa	1	3	1	1	2.0	1.0	2.0
Q9KVV0_VIBCH	VC_0039	SpoOM-related protein	31 kDa	1	3	1	0	2.0	0.5	4.0
Q9KKM0_VIBCH	VC_A1083	LapD subunit	27 kDa	1	3	1	1	2.0	1.0	2.0
Q9KUU6_VIBCH	VC_0419	*cafA*	55 kDa	1	2	0	1	1.5	0.5	3.0
Q9KQD9_VIBCH	VC_2061	ParA	29 kDa	1	3	1	0	2.0	0.5	4.0
Q9KT45_VIBCH	VC_1060	SohB	39 kDa	0	3	0	1	1.5	0.5	3.0
Q9KLZ7_VIBCH	VC_A0592	Putative hydrolase	22 kDa	0	3	1	0	1.5	0.5	3.0
Q9KRN4_VIBCH	VC_1602	CheV	37 kDa	0	3	0	1	1.5	0.5	3.0
Q9KMW3_VIBCH	VC_A0205	*dcuB*	48 kDa	1	3	1	0	2.0	0.5	4.0
Q9KNG2_VIBCH	VC_A0002	*rctB*	75 kDa	2	0	1	0	1.0	0.5	2.0
Q9KVH2_VIBCH	VC_0174	Hypothetical protein	34 kDa	2	0	0	1	1.0	0.5	2.0
Q9KNF7_VIBCH	VC_A0007	3-hydroxyisobutyrate dehydrogenase, putative	33 kDa	0	2	1	0	1.0	0.5	2.0

688

689 **Table V. Cellular proteins that are less abundant in the presence of polymyxin B in *V.***

690 ***cholerae* A1552.**

Accession number	Alternate ID		Molecular weight	PmB 3ug/ml #1	PmB 3ug/ml #2	no PmB #1	No PmB #2	Mean 3µg/ml	Mean No PmB	Ratio 3:0
Q9KQZ3_VIBCH	VC_1854	*ompT*	40 kDa	3	7	25	26	5.0	25.5	0.2
Q9KRP6_VIBCH	VC_1590	AlsS	62 kDa	2	2	4	4	2.0	4.0	0.5
Q9KR21_VIBCH	VC_1826	IIABC mannose permease	66 kDa	1	3	2	8	2.0	5.0	0.4
Q9KM21_VIBCH	VC_A0568	VxrD	42 kDa	0	2	5	5	1.0	5.0	0.2
Q9KS84_VIBCH	VC_1375	Hypothetical protein	27 kDa	0	1	3	1	0.5	2.0	0.3
Q9KL64_VIBCH	VC_A0883	*makA*	39 kDa	1	0	4	4	0.5	4.0	0.1
Q9KLG5_VIBCH	VC_A0779	Fad-dependant oxidoreductase	53 kDa	0	1	3	2	0.5	2.5	0.2
Q9KT68_VIBCH	VC_1037	*mrp*	41 kDa	1	1	4	0	1.0	2.0	0.5
Q9KQJ0_VIBCH	VC_2008	Pyruvate kinase II	52 kDa	1	0	2	0	0.5	1.0	0.5
Q9KTX2_VIBCH	VC_0758	Hypothetical protein	43 kDa	1	0	1	4	0.5	2.5	0.2
Q9KTA5_VIBCH	VC_0998	HubP	178 kDa	0	1	2	1	0.5	1.5	0.3
Q9KUQ6_VIBCH	VC_0459	Hypothetical protein	21 kDa	1	0	1	1	0.5	1.0	0.5
Q9KUT7_VIBCH	VC_0428	*uspA*	16 kDa	1	0	1	3	0.5	2.0	0.3
Q9KPH0_VIBCH	VC_2398	*ftsA*	46 kDa	1	0	2	2	0.5	2.0	0.3
Q9KT65_VIBCH	VC_1040	Corrinoid adenosyl transferase	22 kDa	0	1	1	1	0.5	1.0	0.5
Q9KMF5_VIBCH	VC_A0405	hypothetical protein	23 kDa	1	0	2	2	0.5	2.0	0.3
E5EUX8_VIBCL	VC_A1025	*nagB*	23 kDa	1	0	2	0	0.5	1.0	0.5

691

692

693 **Table VI. Cellular proteins that are only found in the presence of polymyxin B in *V.***

694 ***cholerae* A1552.**

Accession number	Alternate ID		Molecular weight	PmB 3ug/ml #1	PmB 3ug/ml #2	No PmB #1	No PmB #2	Mean 3µg/ml	Mean No PmB
Q9KKN3_VIBCH	VC_A1069	Methyl-accepting chemotaxis protein	70 kDa	6	13	0	0	9.5	0.0
Q9KSD9_VIBCH	VC_1319	VprB	50 kDa	8	11	0	0	9.5	0.0
Q9KKX6_VIBCH	VC_A0974	Methyl-accepting chemotaxis protein	61 kDa	6	8	0	0	7.0	0.0
Q9KV74_VIBCH	VC_0282	Methyl-accepting chemotaxis protein	61 kDa	2	1	0	0	1.5	0.0
Q9KSK4_VIBCH	VC_1252	CinA-like protein	46 kDa	3	7	0	0	5.0	0.0
Q9KQ67_VIBCH	VC_2135	FlrC	52 kDa	2	5	0	0	3.5	0.0
Q9KMZ9_VIBCH	VC_A0167	CalB	29 kDa	2	5	0	0	3.5	0.0
Q9KQ69_VIBCH	VC_2133	FliF	64 kDa	3	7	0	0	5.0	0.0
Q9KP53_VIBCH	VC_2523	Hypothetical protein	35 kDa	2	7	0	0	4.5	0.0
Q9KLR3_VIBCH	VC_A0679	NapB	19 kDa	2	4	0	0	3.0	0.0
Q9KLU7_VIBCH	VC_A0644	NADH oxidase, putative	62 kDa	2	5	0	0	3.5	0.0
Q9KPF1_VIBCH	VC_2417	RecJ	65 kDa	2	4	0	0	3.0	0.0
Q9KQ71_VIBCH	VC_2130	*fliL*	47 kDa	2	2	0	0	2.0	0.0
Q9KNB7_VIBCH	VC_A0048	Hypothetical protein	15 kDa	1	3	0	0	2.0	0.0
Q9KP12_VIBCH	VC_2567	LysM domain-containing protein	22 kDa	1	1	0	0	1.0	0.0
Q9KV14_VIBCH	VC_0344	AmiB	64 kDa	1	1	0	0	1.0	0.0
Q9KTA8_VIBCH	VC_0995	EIIB/EIIC protein	55 kDa	2	1	0	0	1.5	0.0
Q9KSE9_VIBCH	VC_1308	TyrR	58 kDa	2	2	0	0	2.0	0.0
Q9KQM5_VIBCH	VC_1973	*menB*	33 kDa	1	4	0	0	2.5	0.0
Q9KTC9_VIBCH	VC_0973	Hypothetical protein	30 kDa	3	0	0	0	1.5	0.0
Q9KKM3_VIBCH	VC_A1080	LapC	54 kDa	1	2	0	0	1.5	0.0
Q9KTD7_VIBCH	VC_0965	PtsI	63 kDa	1	1	0	0	1.0	0.0
Q9KRR8_VIBCH	VC_1568	VarF	25 kDa	1	1	0	0	1.0	0.0
Q9KUR3_VIBCH	VC_0452	MutY	40 kDa	1	2	0	0	1.5	0.0
Q9KT72_VIBCH	VC_1033	Cation transport ATPase	81 kDa	1	2	0	0	1.5	0.0
Q9KMZ2_VIBCH	VC_A0174	DUF58 domain-containing protein	35 kDa	2	1	0	0	1.5	0.0

695

696

Table VII. Cellular proteins that are only found in absence of polymyxin B in *V. cholerae* A1552.

Accession number	Alternate ID		Molecular weight	PmB 3ug/ml #1	PmB 3ug/ml #2	No PmB #1	No PMB #2	Mean 3µg/ml	Mean No PmB
Q9KSG5_VIBCH	VC_1291	Hypothetical protein	73 kDa	0	0	1	1	0.0	1.0
Q9KQK5_VIBCH	VC_1993	*fadH*	73 kDa	0	0	1	1	0.0	1.0
Q9KVX0_VIBCH	VC_0018	*hspA*	17 kDa	0	0	1	1	0.0	1.0
Q9KKW5_VIBCH	VC_A0985	Oxidoreductase/iron-sulfur cluster-binding protein	105 kDa	0	0	2	1	0.0	1.5

Figures legends

Figure 1. Polymyxin B modifies the proteome of *V. cholerae*. A quantitative proteomic analysis by liquid chromatography coupled to mass spectrometry of *V. cholerae* A1552 grown in Type VI Secretion System activating conditions, with or without 3 µg/ml of Polymyxin B (PmB) was performed. Scatter plot analysis using the total number of spectra per protein was performed to determine the correlation between the biological duplicates of the sample without PmB **(A)** and with 3 µg/ml of PmB **(B)**. A GoAnnotation analysis of the proteins identified determined the molecular functions, implication in biological processes and localization of the proteins **(C)**.

Figure 2. Normalized relative expression of known T6SS regulators (A) and structural components (B) in *V. cholerae* grown with polymyxin B. *V. cholerae* A1552 was grown to midlog phase in LB2%NaCl supplemented or not with 3 µg/ml of polymyxin B (PmB). Total RNA was extracted from cultures and retrotranscribed. The expression of selected regulators and structural components was measured by quantitative PCR in the presence of PmB in comparison to the non-treated cells, and normalized using *recA*. Data represent mean ± SD of

three independent experiments conducted in triplicates. Asterisk represents a significant difference in expression between treated and non-treated cells ($P<0.05$). CRP, cyclic AMP receptor protein.

Figure 3. The two-component system VxrAB plays a role in *hcp* upregulation in *V. cholerae* in the presence of subinhibitory concentrations of polymyxin B. *V. cholerae* A1552 and A1552Δ*vxrAB*::CmR (A1552Δ*vxrAB*) were grown to midlog phase in LB2%NaCl with or without 3 µg/ml of polymyxin B (PmB). Total RNA was extracted from cultures and retrotranscribed. The expression of *hcp1* **(A)** or *hcp2* **(B)** was measured by quantitative PCR in the presence of PmB in comparison to the non-treated cells, and normalized using *recA*. Data represent mean ± SD of three independent experiments conducted in triplicates. Asterisk represents a significant difference in expression between treated and non-treated cells ($P<0.05$). ns, non-significative difference. **C)** The complementation of *vxrAB* restores the level of Hcp in the supernatant of A1552Δ*vxrAB*::CmR pBAD24-*vxrAB*. A1552 pBAD24, A1552Δ*vxrAB*::CmR pBAD24 and A1552Δ*vxrAB*::CmR pBAD24-*vxrAB* were grown to late exponential phase in LB-2%NaCl in the presence of PmB.

– FIGURES –

Comprehension of Antimicrobial Peptides Modulation of the Type VI Secretion System in *Vibrio cholerae*

Annabelle Mathieu-Denoncourt and Marylise Duperthuy*.

Département de Microbiologie, infectiologie et immunologie, Faculté de médecine, Université de Montréal, Montréal, H3T 1J4, Quebec, Canada.

*Corresponding author: Marylise Duperthuy, Université de Montréal, C.P. 6128, succursale Centre-ville, Montréal, QC, H3C 3J7, tel : 514 343-6111, fax: 514 343-5701, marylise.duperthuy@umontreal.ca

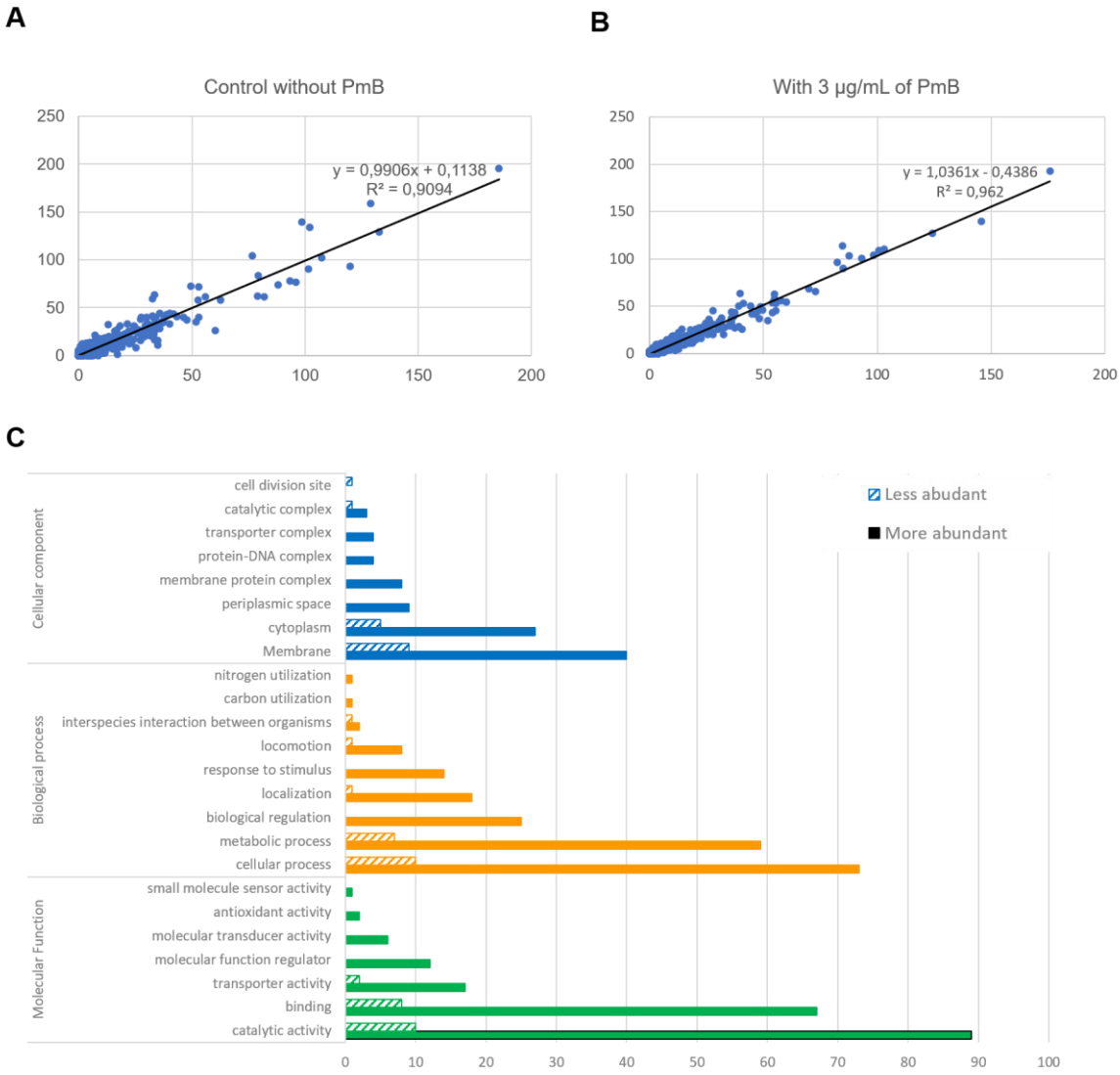

Figure 1. Polymyxin B modifies the proteome of *V. cholerae*. A quantitative proteomic analysis by liquid chromatography coupled to mass spectrometry of *V. cholerae* A1552 grown in Type VI Secretion System activating conditions, with or without 3 µg/ml of Polymyxin B (PmB) was performed. Scatter plot analysis using the total number of spectra per protein was performed to determine the correlation between the biological duplicates of the sample without PmB **(A)** and with 3 µg/ml of PmB **(B)**. A GoAnnotation analysis of the proteins identified determined the molecular functions, implication in biological processes and localization of the proteins **(C)**.

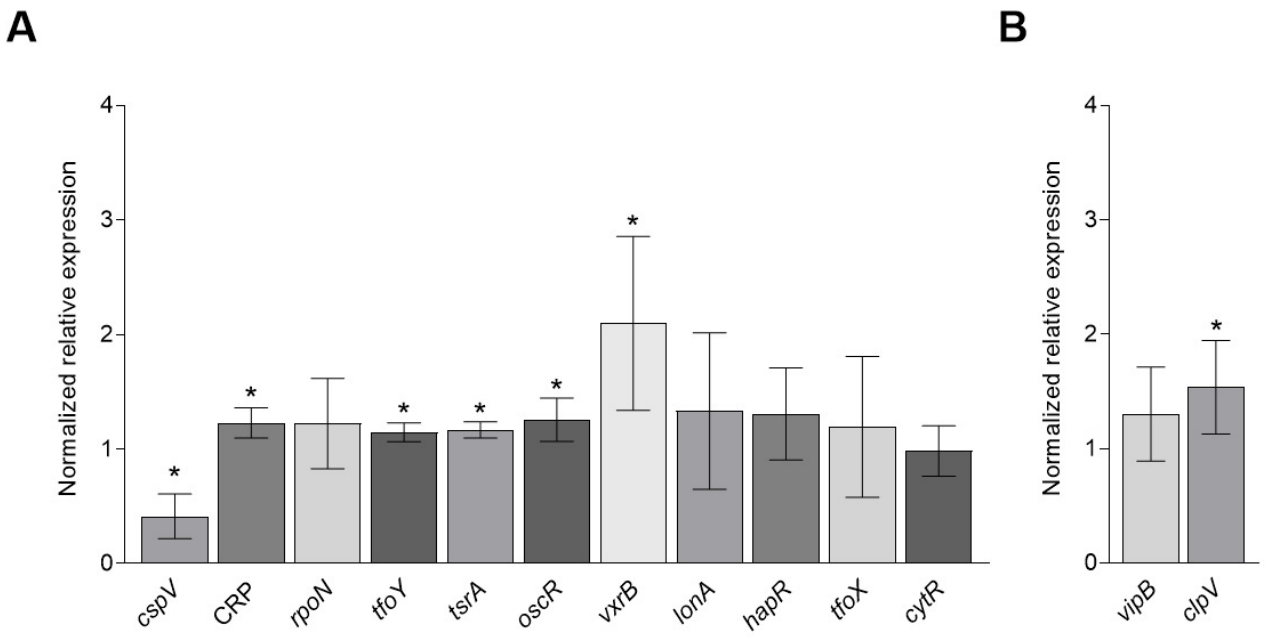

Figure 2. Normalized relative expression of known T6SS regulators (A) and structural components (B) in *V. cholerae* grown with polymyxin B. *V. cholerae* A1552 was grown to midlog phase in LB2%NaCl supplemented or not with 3 µg/ml of polymyxin B (PmB). Total RNA was extracted from cultures and retrotranscribed. The expression of selected regulators and structural components was measured by quantitative PCR in the presence of PmB in comparison to the non-treated cells, and normalized using *recA*. Data represent mean ± SD of three independent experiments conducted in triplicates. Asterisk represents a significant difference in expression between treated and non-treated cells (P<0.05). CRP, cyclic AMP receptor protein.

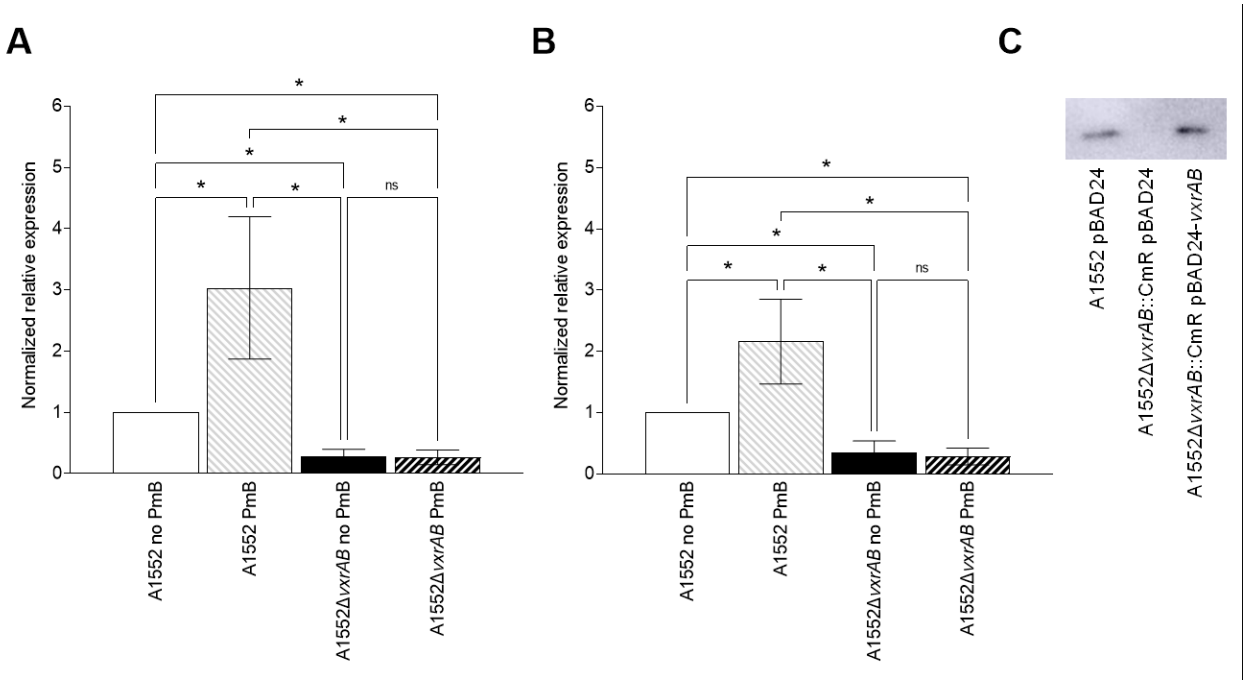

Figure 3. The two-component system VxrAB plays a role in *hcp* upregulation in *V. cholerae* in the presence of subinhibitory concentrations of polymyxin B. *V. cholerae* A1552 and A1552Δ*vxrAB*::CmR (A1552Δ*vxrAB*) were grown to midlog phase in LB2%NaCl with or without 3 µg/ml of polymyxin B (PmB). Total RNA was extracted from cultures and retrotranscribed. The expression of *hcp1* **(A)** or *hcp2* **(B)** was measured by quantitative PCR in the presence of PmB in comparison to the non-treated cells, and normalized using *recA*. Data represent mean ± SD of three independent experiments conducted in triplicates. Asterisk represents a significant difference in expression between treated and non-treated cells ($P<0.05$). ns, non-significative difference. **C)** The complementation of *vxrAB* restores the level of Hcp in the supernatant of A1552Δ*vxrAB*::CmR pBAD24-*vxrAB*. A1552 pBAD24, A1552Δ*vxrAB*::CmR pBAD24 and A1552Δ*vxrAB*::CmR pBAD24-*vxrAB* were grown to late exponential phase in LB-2%NaCl in the presence of PmB.